Convergence of the generalized-α scheme for constrained mechanical systems

Martin Arnold[1] and Olivier Brüls[2]

[1]NWF III - Institute of Mathematics

Martin Luther University Halle-Wittenberg

D - 06099 Halle (Saale), Germany

martin.arnold@mathematik.uni-halle.de

[2]Department of Aerospace and Mechanical Engineering

University of Liège

B - 4000 Liège, Belgium

o.bruls@ulg.ac.be

Abstract

A variant of the generalized-α scheme is proposed for constrained mechanical systems represented by index-3 DAEs. Based on the analogy with linear multistep methods, an elegant convergence analysis is developed for this algorithm. Second-order convergence is demonstrated both for the generalized coordinates and the Lagrange multipliers, and those theoretical results are illustrated by numerical tests.

Key-words : DAEs, generalized-α method

1 Introduction

The generalized-α scheme has been initially developed for the simulation of finite element models in structural dynamics. It allows a simple and efficient implementation as well as an optimal combination of accuracy at low-frequency and numerical damping at high-frequency. This last feature is especially interesting since it allows to eliminate the contribution of non-physical high-frequency modes, which are generally present in finite element models. The generalized-α algorithm results from successive contributions by Newmark [18], Hilber, Hughes and Taylor [14], and Chung and Hulbert [9]; an overview of its properties in the nonlinear regime is also given by Erlicher et al [10].

This work concerns the employment of the generalized-α scheme for the simulation of constrained mechanical systems. Cardona and Géradin [8] have shown that numerical damping is critical to avoid numerical oscillations in the Lagrange multipliers. Their theoretical investigations are restricted to linear problems, but they also report consistent results in nonlinear test cases. However, it is well-known that the order of an integration algorithm can be reduced due to the presence of algebraic constraints [4, 13], which calls for a rigorous convergence analysis of the generalized-α method in the context of differential-algebraic systems. Recently, Lunk and Simeon [16] and Jay and Negrut [15] have proven second-order convergence for regularized index-2 formulations, i.e. algorithms which make use of kinematic constraints at both position and velocity level.

In contrast, an algorithm based on an index-3 formulation, i.e. solely based on position level constraints, is analysed in this paper. This algorithm can deal with a non-constant mass

matrix and it computes the acceleration variables with second-order accuracy. It extends the approach of Negrut et al [17] who report on positive practical experience with the Hilber–Hughes–Taylor algorithm applied to the index-3 formulation of the equations of motion in an industrial multibody system simulation tool. Recently, Bottasso et al [3] proposed a scaling technique to reduce the numerical instability effects being typical of such time integration methods for DAEs of index 3, see [1, 2, 4].

In the present paper, the analogy between generalized-α algorithms and linear multistep integrators helps to get a simpler and more intuitive convergence proof, see also the rather technical work of Lunk and Simeon [16] or Jay and Negrut [15]. Second-order convergence is demonstrated both for the generalized coordinates and the Lagrange multipliers. The remaining part of the paper is organized as follows: the generalized-α algorithm and its multistep representation are introduced in Section 2. Estimates for local and global errors are proven in Section 3. Some technical parts of the proof are collected separately in Section 4. In Section 5, the results of the theoretical investigations are illustrated by numerical tests. The conclusions in Section 6 summarize essential parts of the paper.

2 The generalized-α method

Let us consider the constrained mechanical system

$$\mathbf{M}(\mathbf{q})\ddot{\mathbf{q}} \;=\; \mathbf{f}(\mathbf{q},\dot{\mathbf{q}},t) - \mathbf{\Phi}_{\mathbf{q}}^{T}\boldsymbol{\lambda}, \tag{1}$$

$$\mathbf{0} \;=\; \mathbf{\Phi}(\mathbf{q},t) \tag{2}$$

where Equation (1) represents the dynamics of the mechanical system and Equation (2) represents the kinematic constraints. The vectors $\mathbf{q}$ and $\boldsymbol{\lambda}$ denote the generalized coordinates and the Lagrange multipliers, respectively, $\mathbf{M}$ is the symmetric mass matrix, the vector of apparent forces $\mathbf{f}$ collects external forces, internal forces and complementary inertia forces, and $\mathbf{\Phi}_{\mathbf{q}}$ is the matrix of constraint gradients. The mass matrix is not necessarily constant but it may depend on the generalized coordinates $\mathbf{q}$, which allows to cover the case of mechanical systems with large rotations. We note that the present developments could be further extended to mechatronic problems, as suggested by Bruls and Golinval [6, 7].

2.1 Description of the algorithm

We propose an implementation of the generalized-α method which does not rely on a weighted formulation of the residual equation. Instead, the dynamic equilibrium is enforced exactly at every time step, with three major advantages: (i) the accelerations are computed with second-order accuracy, (ii) the consistency of the algorithm is not affected if the mass matrix is not constant, (iii) the algorithm is closer to the physics of the problem, which also simplifies theoretical investigations.

Hence, the numerical variables $\mathbf{q}_{n+1}$, $\dot{\mathbf{q}}_{n+1}$, $\ddot{\mathbf{q}}_{n+1}$, $\boldsymbol{\lambda}_{n+1}$ satisfy Equations (1)-(2) at time $t = t_{n+1}$, whereas the vector $\mathbf{a}$ of acceleration-like variables is defined by the recurrence relation

$$(1-\alpha_m)\mathbf{a}_{n+1} + \alpha_m\mathbf{a}_n = (1-\alpha_f)\ddot{\mathbf{q}}_{n+1} + \alpha_f\ddot{\mathbf{q}}_n, \qquad \mathbf{a}_0 = \ddot{\mathbf{q}}_0. \tag{3}$$

We emphasize that $\mathbf{a}$ is an auxiliary variable, which is not equal to the true accelerations $\ddot{\mathbf{q}}$. Since $\mathbf{M}$ depends on $\mathbf{q}$, this equation cannot be restated as a weighted form of Equation (1). The generalized-α scheme is obtained using $\mathbf{a}$ in the Newmark integration formulae

$$\mathbf{q}_{n+1} \;=\; \mathbf{q}_n + h\dot{\mathbf{q}}_n + h^2(\frac{1}{2}-\beta)\mathbf{a}_n + h^2\beta\mathbf{a}_{n+1}, \tag{4}$$

$$\dot{\mathbf{q}}_{n+1} \;=\; \dot{\mathbf{q}}_n + h(1-\gamma)\mathbf{a}_n + h\gamma\mathbf{a}_{n+1} \tag{5}$$

where h is the step-size. The numerical parameters α_m, α_f, β and γ can be selected in order to have suitable accuracy and stability properties.

Algorithm 1 solves formulae (3), (4), (5) together with the dynamic equilibrium at time t_{n+1}. The correction step involves the parameters

$$\beta' = \frac{1 - \alpha_m}{h^2 \beta (1 - \alpha_f)}, \qquad \gamma' = \frac{\gamma}{h\beta} \tag{6}$$

which satisfy the properties

$$\frac{\partial \ddot{\mathbf{q}}_{n+1}}{\partial \mathbf{q}_{n+1}} = \mathbf{I}\beta', \qquad \frac{\partial \dot{\mathbf{q}}_{n+1}}{\partial \mathbf{q}_{n+1}} = \mathbf{I}\gamma'. \tag{7}$$

Moreover, the iteration matrix is given by

$$\mathbf{S}_t = \left[\begin{array}{cc} (\mathbf{M}\beta' + \mathbf{C}_t\gamma' + \mathbf{K}_t) & \mathbf{\Phi}_{\mathbf{q}}^T \\ \mathbf{\Phi}_{\mathbf{q}} & \mathbf{0} \end{array} \right]$$

with the tangent stiffness matrix $\mathbf{K}_t = \partial(\mathbf{M}\ddot{\mathbf{q}} - \mathbf{f} + \mathbf{\Phi}_{\mathbf{q}}^T\boldsymbol{\lambda})/\partial\mathbf{q}$ and the tangent damping matrix $\mathbf{C}_t = \partial(-\mathbf{f})/\partial\dot{\mathbf{q}}$. Compared to a classical algorithm based on a weighted formulation of Equation (1), as described in [9, 14], Algorithm 1 involves similar computational resources. Indeed, it only requires one additional vector $\mathbf{a}$, and the correction step, which is the most demanding part of the algorithm, is barely modified.

Algorithm 1 $[\mathbf{q}_{n+1}, \dot{\mathbf{q}}_{n+1}, \ddot{\mathbf{q}}_{n+1}, \boldsymbol{\lambda}_{n+1}, \mathbf{a}]$ = `AlphaStep`$(\mathbf{q}_n, \dot{\mathbf{q}}_n, \ddot{\mathbf{q}}_n, \mathbf{a})$

$\quad \mathbf{q}_{n+1} := \mathbf{q}_n + h\dot{\mathbf{q}}_n + h^2(0.5 - \beta)\mathbf{a}$
$\quad \dot{\mathbf{q}}_{n+1} := \dot{\mathbf{q}}_n + h(1 - \gamma)\mathbf{a}$
$\quad \boldsymbol{\lambda}_{n+1} := \mathbf{0}$
$\quad \mathbf{a} := 1/(1 - \alpha_m)(\alpha_f \ddot{\mathbf{q}}_n - \alpha_m \mathbf{a})$
$\quad \mathbf{q}_{n+1} := \mathbf{q}_{n+1} + h^2\beta\mathbf{a}$
$\quad \dot{\mathbf{q}}_{n+1} := \dot{\mathbf{q}}_{n+1} + h\gamma\mathbf{a}$
$\quad \ddot{\mathbf{q}}_{n+1} := \mathbf{0}$
$\quad$ **for** $i = 1$ to i_{max} **do**
$\quad\quad$ Compute the residuals $\mathbf{r}^{\mathbf{q}}$ (Equation (1)), $\mathbf{r}^{\boldsymbol{\lambda}}$ (Equation (2))
$\quad\quad$ **if** $\sqrt{\|\mathbf{r}^{\mathbf{q}}\|^2 + \|\mathbf{r}^{\boldsymbol{\lambda}}\|^2} < tol$ **then**
$\quad\quad\quad$ break
$\quad\quad$ **end if**
$\quad\quad \left[\begin{array}{c} \Delta\mathbf{q} \\ \Delta\boldsymbol{\lambda} \end{array} \right] := -\mathbf{S}_t^{-1} \left[\begin{array}{c} \mathbf{r}^{\mathbf{q}} \\ \mathbf{r}^{\boldsymbol{\lambda}} \end{array} \right]$
$\quad\quad \mathbf{q}_{n+1} := \mathbf{q}_{n+1} + \Delta\mathbf{q}$
$\quad\quad \dot{\mathbf{q}}_{n+1} := \dot{\mathbf{q}}_{n+1} + \gamma'\Delta\mathbf{q}$
$\quad\quad \ddot{\mathbf{q}}_{n+1} := \ddot{\mathbf{q}}_{n+1} + \beta'\Delta\mathbf{q}$
$\quad\quad \boldsymbol{\lambda}_{n+1} := \boldsymbol{\lambda}_{n+1} + \Delta\boldsymbol{\lambda}$
$\quad$ **end for**
$\quad \mathbf{a} := \mathbf{a} + (1 - \alpha_f)/(1 - \alpha_m)\ddot{\mathbf{q}}_{n+1}$

For small time steps h, the matrix $\mathbf{S}_t$ becomes severely ill conditioned. Bottasso et al [3] have proposed a scaling method in order to avoid this phenomenon, see also the closely related scaling approach of Hairer and Wanner [13] in the classical general purpose DAE solver RADAU5. The linear system

$$\mathbf{S}_t\mathbf{x} = -\mathbf{r}, \tag{8}$$

with $\mathbf{x}^T = [\Delta\mathbf{q}^T \; \Delta\boldsymbol{\lambda}^T]$ and $\mathbf{r}^T = [(\mathbf{r}^{\mathbf{q}})^T \; (\mathbf{r}^{\boldsymbol{\lambda}})^T]$ is replaced by the equivalent scaled form

$$\overline{\mathbf{S}}_t\overline{\mathbf{x}} = -\overline{\mathbf{r}} \tag{9}$$

with $\overline{\mathbf{S}}_t = \mathbf{D}_L\mathbf{S}_t\mathbf{D}_R$, $\overline{\mathbf{x}} = \mathbf{D}_R^{-1}\mathbf{x}$ and $\overline{\mathbf{r}} = \mathbf{D}_L\mathbf{r}$. In the numerical tests presented in Section 5, the diagonal left and right preconditioners

$$\mathbf{D}_L = \left[\begin{array}{cc} \mathbf{I}\beta h^2 & \mathbf{0} \\ \mathbf{0} & \mathbf{I} \end{array} \right], \qquad \mathbf{D}_R = \left[\begin{array}{cc} \mathbf{I} & \mathbf{0} \\ \mathbf{0} & \mathbf{I}/\beta h^2 \end{array} \right] \tag{10}$$

are used to achieve an optimal conditioning of the matrix $\overline{\mathbf{S}}_t$, see [3].

2.2 Multistep representation of the algorithm

Assuming that the mass matrix is non-singular, the dynamic equilibrium is equivalent to an explicit form

$$\ddot{\mathbf{q}} = \mathbf{g}(\mathbf{q}, \dot{\mathbf{q}}, \boldsymbol{\lambda}, t), \tag{11}$$
$$\mathbf{0} = \boldsymbol{\Phi}(\mathbf{q}, t) \tag{12}$$

with $\mathbf{g} = \mathbf{M}^{-1}(\mathbf{f} - \boldsymbol{\Phi}_{\mathbf{q}}^T \boldsymbol{\lambda})$. We also assume that the constrained system (11)-(12) has DAE index 3, i.e. that the matrix

$$\boldsymbol{\Phi}_{\mathbf{q}} \mathbf{g}_{\boldsymbol{\lambda}} \tag{13}$$

is non-singular, where $\mathbf{g}_{\boldsymbol{\lambda}}$ is given by $\mathbf{g}_{\boldsymbol{\lambda}} = -\mathbf{M}^{-1}\boldsymbol{\Phi}_{\mathbf{q}}^T$. Since the dynamic equilibrium is enforced at every time step, the algorithm leads to the same solution when applied to the system (11)-(12) and it is sufficient to analyse this equivalent system.

It is possible to eliminate $\mathbf{a}$ from the integration formulae at time steps $t_{n-1} \to t_n$ and $t_n \to t_{n+1}$, leading to a two-step formulation [10]

$$\sum_{k=0}^{2} a_k \mathbf{q}_{n+k-1} + h \sum_{k=0}^{1} u_k \dot{\mathbf{q}}_{n+k-1} = h^2 \sum_{k=0}^{2} b_k \mathbf{g}_{n+k-1}, \tag{14}$$

$$\sum_{k=0}^{2} a_k \dot{\mathbf{q}}_{n+k-1} = h \sum_{k=0}^{2} c_k \mathbf{g}_{n+k-1}, \tag{15}$$

$$\mathbf{0} = \boldsymbol{\Phi}(\mathbf{q}_{n+1}, t_{n+1}) \tag{16}$$

with the coefficients

$$
\begin{array}{lll}
a_0 = -\alpha_m, & a_1 = -1 + 2\alpha_m, & a_2 = 1 - \alpha_m, \\
u_0 = -\alpha_m, & u_1 = -1 + \alpha_m, & \\
b_0 = \alpha_f(1/2 - \beta), & b_1 = (1 - \alpha_f)(1/2 - \beta) + \alpha_f \beta, & b_2 = (1 - \alpha_f)\beta, \\
c_0 = \alpha_f(1 - \gamma), & c_1 = (1 - \alpha_f)(1 - \gamma) + \alpha_f \gamma, & c_2 = (1 - \alpha_f)\gamma.
\end{array}
$$

In Section 3 below, we will see that the detailed analysis of the error propagation in the difference quotients

$$\mathbf{q}_n' := \frac{\mathbf{q}_n - \mathbf{q}_{n-1}}{h} \approx \dot{\mathbf{q}}(t_n - \frac{h}{2}) \tag{17}$$

is very useful to study the error propagation for the Lagrange multipliers $\boldsymbol{\lambda}$. A two-step recursion for $\mathbf{q}'$ is obtained by the difference quotient of Equation (14) in its original form and Equation (14) with n being substituted by $n - 1$. In this difference quotient, the velocities $\dot{\mathbf{q}}$ may be eliminated using Equation (15) resulting finally in the multistep formula

$$\sum_{k=0}^{2} a_k \mathbf{q}_{n+k-1}' = h \sum_{k=0}^{3} b_k' \mathbf{g}_{n+k-2} \tag{18}$$

with coefficients

$$
\begin{array}{ll}
b_0' = \alpha_f(1/2 + \beta - \gamma), & b_1' = (1 - \alpha_f)(1/2 + \beta - \gamma) + \alpha_f(1/2 - 2\beta + \gamma), \\
b_2' = (1 - \alpha_f)(1/2 - 2\beta + \gamma) + \alpha_f \beta, & b_3' = (1 - \alpha_f)\beta.
\end{array} \tag{19}
$$

2.3 Choice of the numerical parameters

In the present paper, generalized-α algorithms with fixed step-sizes h are considered. In that case, the generalized-α algorithm for unconstrained mechanical systems is second-order accurate provided that [9]

$$\gamma = \frac{1}{2} + \alpha_f - \alpha_m. \tag{20}$$

Note, however, that this condition is no more valid for variable step-size algorithms and should be replaced by an update condition for the parameter γ, which means that the value of γ should be adapted at each time step to guarantee second-order accuracy [5].

The numerical solution is zero-stable (i.e. stable for $h \to 0$) if the polynomial

$$\varrho(\zeta) := \sum_{k=0}^{2} a_k \zeta^k \tag{21}$$

satisfies the root condition, i.e., if condition $|\zeta_i| \leq 1$ is satisfied for all roots ζ_i, $i = 1, 2$ of polynomial ϱ. For multiple roots ζ_i, the stronger condition $|\zeta_i| < 1$ has to be enforced [12]. Since the roots of ϱ are $\zeta_1 = 1$ and $\zeta_2 = -\alpha_m/(1 - \alpha_m)$, zero stability requires $\alpha_m \leq 0.5$. We note that both roots are necessarily simple.

The algorithm is strictly stable at infinity (i.e. strictly stable for $h \to \infty$, see [13]) if all roots ζ_i' of the polynomial

$$\sigma(\zeta) := \sum_{k=0}^{3} b_k' \zeta^k \tag{22}$$

satisfy $|\zeta_i'| < 1$, $i = 1, 2, 3$. Lemma 1, see Section 4 below, shows that strict stability at infinity is guaranteed if

$$\alpha_m < \alpha_f < \frac{1}{2}, \quad \beta > \frac{1}{4} + \frac{1}{2}(\alpha_f - \alpha_m) \tag{23}$$

and the order 2 condition (20) is satisfied.

For stiff problems, the numerical solution should be computed accurately only in the low-frequency range, whereas the high-frequency response should rather be damped out by the algorithm. The high-frequency numerical damping is represented by the spectral radius of the algorithm at infinity ρ_∞: an undamped scheme is characterized by $\rho_\infty = 1$, whereas $\rho_\infty = 0$ means asymptotic annihilation of the high-frequency response. For a given value of $\rho_\infty \in [0, 1]$, Chung and Hulbert [9] have proposed optimal algorithmic parameters for second-order ODEs

$$\alpha_m = \frac{2\rho_\infty - 1}{\rho_\infty + 1}, \quad \alpha_f = \frac{\rho_\infty}{\rho_\infty + 1}, \quad \beta = \frac{1}{4}\left(\gamma + \frac{1}{2}\right)^2 \tag{24}$$

whereas γ is computed according to (20). For $\rho_\infty \in [0, 1)$, the resulting algorithms are both zero-stable and strictly stable at infinity. Indeed, $\rho_\infty < 1$ implies

$$\alpha_m < \alpha_f < \frac{1}{2}, \quad \gamma > \frac{1}{2}$$

and

$$\beta = \frac{1}{4}\left(\gamma + \frac{1}{2}\right)^2 > \frac{1}{4}\left(\gamma + \frac{1}{2}\right)^2 - \frac{1}{4}\left(\gamma - \frac{1}{2}\right)^2 = \frac{1}{2}\gamma = \frac{1}{4} + \frac{1}{2}(\alpha_f - \alpha_m),$$

so that both conditions in Equation (23) are satisfied.

3 Convergence analysis

3.1 Local truncation error

By definition, the method is *convergent of order 2* in the classical unconstrained case if $\|\mathbf{q}(t_n) - \mathbf{q}_n\|$ and $\|\dot{\mathbf{q}}(t_n) - \dot{\mathbf{q}}_n\|$ are $\mathcal{O}(h^2)$. In contrast, the *order 2 condition* (Equation (20)) means that

the local error, i.e. the error after one time step, is $\mathcal{O}(h^3)$. It can be demonstrated [12] that this last condition is satisfied iff $\mathbf{l}_n^{\mathbf{q}}$ and $\mathbf{l}_n^{\dot{\mathbf{q}}}$ are $\mathcal{O}(h^3)$, where the local truncation errors $\mathbf{l}_n^{\mathbf{q}}$ and $\mathbf{l}_n^{\dot{\mathbf{q}}}$ are defined by introducing the exact solution $\mathbf{q}(t_n)$, $\dot{\mathbf{q}}(t_n)$, $\boldsymbol{\lambda}(t_n)$ into Equations (14) and (15)

$$\mathbf{l}_n^{\mathbf{q}} = \sum_{k=0}^{2} a_k \mathbf{q}(t_{n+k-1}) + h \sum_{k=0}^{1} u_k \dot{\mathbf{q}}(t_{n+k-1}) - h^2 \sum_{k=0}^{2} b_k \mathbf{g}(t_{n+k-1}), \tag{25}$$

$$\mathbf{l}_n^{\dot{\mathbf{q}}} = \sum_{k=0}^{2} a_k \dot{\mathbf{q}}(t_{n+k-1}) - h \sum_{k=0}^{2} c_k \mathbf{g}(t_{n+k-1}) \tag{26}$$

with the notation $\mathbf{g}(t_n) = \mathbf{g}(\mathbf{q}(t_n), \dot{\mathbf{q}}(t_n), \boldsymbol{\lambda}(t_n), t_n)$.

For the extension of these results to the constrained case, see Equations (11)-(12), we consider furthermore the local truncation error $\mathbf{l}_n^{\mathbf{q}'}$ in Equation (18):

$$\mathbf{l}_n^{\mathbf{q}'} = \sum_{k=0}^{2} a_k \frac{\mathbf{q}(t_{n+k-1}) - \mathbf{q}(t_{n+k-2})}{h} - h \sum_{k=0}^{3} b_k' \mathbf{g}(t_{n+k-2}). \tag{27}$$

The classical order 2 condition in Equation (20) implies that the new consistency conditions

$$\sum_{k=0}^{2} a_k = 0 \quad \text{and} \quad \frac{1}{(j+1)!} \sum_{k=0}^{2} a_k \left((k-1)^{j+1} - (k-2)^{j+1} \right) = \frac{1}{(j-1)!} \sum_{k=0}^{3} b_k' (k-2)^{j-1}, \ (j=1,2)$$

are satisfied and the estimate $\|\mathbf{l}_n^{\mathbf{q}'}\| = \mathcal{O}(h^3)$ may be shown by Taylor expansion.

3.2 Error propagation in the differential solution components

When a zero-stable algorithm is used to solve an ODE, the order condition implies global convergence [12]. The extension of this classical result from the ODE case to the constrained system in Equations (11)-(12), i.e. to index-3 DAEs, follows the basic lines of the convergence analysis for multistep methods applied to DAEs, see [13].

In a first step, let us analyse the error propagation during the integration process for the differential components $\mathbf{q}$, $\dot{\mathbf{q}}$ and $\mathbf{q}'$. Using the multistep formulae (14), (15) and (18), the defect Equations (25), (26) and (27) become

$$\mathbf{l}_n^{\mathbf{q}} = \sum_{k=0}^{2} a_k \mathbf{e}_{n+k-1}^{\mathbf{q}} + h \sum_{k=0}^{1} u_k \mathbf{e}_{n+k-1}^{\dot{\mathbf{q}}} - h^2 \sum_{k=0}^{2} b_k \mathbf{e}_{n+k-1}^{\mathbf{g}}, \tag{28}$$

$$\mathbf{l}_n^{\dot{\mathbf{q}}} = \sum_{k=0}^{2} a_k \mathbf{e}_{n+k-1}^{\dot{\mathbf{q}}} - h \sum_{k=0}^{2} c_k \mathbf{e}_{n+k-1}^{\mathbf{g}}, \tag{29}$$

$$\mathbf{l}_n^{\mathbf{q}'} = \sum_{k=0}^{2} a_k \mathbf{e}_{n+k-1}^{\mathbf{q}'} - h \sum_{k=0}^{3} b_k' \mathbf{e}_{n+k-2}^{\mathbf{g}} \tag{30}$$

where $\mathbf{e}_n^{(\bullet)} = (\bullet)(t_n) - (\bullet)_n$ represent a global error after n steps and

$$\mathbf{e}_n^{\mathbf{q}'} := \frac{\mathbf{q}(t_n) - \mathbf{q}(t_{n-1})}{h} - \frac{\mathbf{q}_n - \mathbf{q}_{n-1}}{h} = \frac{\mathbf{e}_n^{\mathbf{q}} - \mathbf{e}_{n-1}^{\mathbf{q}}}{h}, \tag{31}$$

see Equation (17). Inspired by the identical structure of the first terms in the right hand sides of Equations (28)-(30), the three differential components $\mathbf{q}$, $\dot{\mathbf{q}}$ and $\mathbf{q}'$ and the corresponding local and global errors are summarized in

$$\mathbf{v}(t_n) := \begin{pmatrix} \mathbf{q}(t_n) \\ \dot{\mathbf{q}}(t_n) \\ \mathbf{q}'(t_n) \end{pmatrix}, \quad \mathbf{v}_n := \begin{pmatrix} \mathbf{q}_n \\ \dot{\mathbf{q}}_n \\ \mathbf{q}_n' \end{pmatrix}, \quad \mathbf{e}_n^{\mathbf{v}} := \begin{pmatrix} \mathbf{e}_n^{\mathbf{q}} \\ \mathbf{e}_n^{\dot{\mathbf{q}}} \\ \mathbf{e}_n^{\mathbf{q}'} \end{pmatrix}, \quad \mathbf{l}_n^{\mathbf{v}} := \begin{pmatrix} \mathbf{l}_n^{\mathbf{q}} \\ \mathbf{l}_n^{\dot{\mathbf{q}}} \\ \mathbf{l}_n^{\mathbf{q}'} \end{pmatrix} = \mathcal{O}(h^3). \tag{32}$$

With this compact notation, the error recursion defined by Equations (28)-(30) may be written as

$$
\begin{aligned}
\mathbf{e}_{n+1}^{\mathbf{v}} &= -\frac{a_0}{a_2}\mathbf{e}_{n-1}^{\mathbf{v}} - \frac{a_1}{a_2}\mathbf{e}_n^{\mathbf{v}} + \mathcal{O}(h)\sum_{k=0}^{1}\|\mathbf{e}_{n+k-1}^{\dot{\mathbf{q}}}\| + \mathcal{O}(h)\sum_{k=0}^{3}\|\mathbf{e}_{n+k-2}^{\mathbf{g}}\| + \mathcal{O}(h^3) \\
&= -\frac{a_0}{a_2}\mathbf{e}_{n-1}^{\mathbf{v}} - \frac{a_1}{a_2}\mathbf{e}_n^{\mathbf{v}} + \mathcal{O}(h)\sum_{k=0}^{3}(\|\mathbf{e}_{n+k-2}^{\mathbf{v}}\| + \|\mathbf{e}_{n+k-2}^{\boldsymbol{\lambda}}\|) + \mathcal{O}(h^3)\,. \quad (33)
\end{aligned}
$$

The propagation of the errors $\mathbf{e}_n^{\mathbf{q}}$, $\mathbf{e}_n^{\dot{\mathbf{q}}}$ and $\mathbf{e}_n^{\mathbf{q}'}$ is dominated by the recursion coefficients a_0, a_1 and a_2 and it is coupled with the errors $\mathbf{e}_n^{\boldsymbol{\lambda}}$ in the algebraic components $\boldsymbol{\lambda}$ by $\mathcal{O}(h)$ coupling coefficients.

3.3 Error propagation in the algebraic solution components

For the analysis of the error propagation in the algebraic solution components $\boldsymbol{\lambda}$, we assume that throughout integration the numerical solution $(\mathbf{q}_n, \dot{\mathbf{q}}_n, \boldsymbol{\lambda}_n)$ remains in a small neighbourhood of the analytical solution $(\mathbf{q}(t_n), \dot{\mathbf{q}}(t_n), \boldsymbol{\lambda}(t_n))$:

$$
\|\mathbf{e}_n^{\mathbf{q}}\| \le Ch\,, \quad \|\mathbf{e}_n^{\dot{\mathbf{q}}}\| \le Ch\,, \quad \|\mathbf{e}_n^{\boldsymbol{\lambda}}\| \le Ch\,, \ (n \ge 0) \quad (34)
$$

with a constant $C > 0$ that is independent of n and h.

Because of the $\mathcal{O}(h^2)$ error bounds for $\|\mathbf{e}_n^{\mathbf{q}}\|$, $\|\mathbf{e}_n^{\dot{\mathbf{q}}}\|$, $\|\mathbf{e}_n^{\boldsymbol{\lambda}}\|$ in Equation (41) below, the additional assumption in Equation (34) is always satisfied if $h > 0$ is sufficiently small and the initial values of the numerical solution are sufficiently close to the analytical solution, see also part c) of the proof of Theorem VII.3.5 in [13] for a more detailed discussion.

The conditions on $\|\mathbf{e}_n^{\mathbf{q}}\|$, $\|\mathbf{e}_n^{\dot{\mathbf{q}}}\|$, $\|\mathbf{e}_n^{\boldsymbol{\lambda}}\|$ in Equation (34) allow to get an estimate for $\sum_k b_k' \mathbf{e}_{n+k-2}^{\boldsymbol{\lambda}}$ from Equation (30). With

$$
\boldsymbol{\psi}(\vartheta) := \mathbf{g}(\mathbf{q}_{n+k-2} + \vartheta \mathbf{e}_{n+k-2}^{\mathbf{q}}, \dot{\mathbf{q}}_{n+k-2} + \vartheta \mathbf{e}_{n+k-2}^{\dot{\mathbf{q}}}, \boldsymbol{\lambda}_{n+k-2} + \vartheta \mathbf{e}_{n+k-2}^{\boldsymbol{\lambda}}, t_{n+k-2})
$$

we have

$$
\begin{aligned}
\mathbf{e}_{n+k-2}^{\mathbf{g}} = \boldsymbol{\psi}(1) - \boldsymbol{\psi}(0) &= \int_0^1 \boldsymbol{\psi}'(\vartheta)\,\mathrm{d}\vartheta = \\
&= \int_0^1 \mathbf{g}_{\boldsymbol{\lambda}}(\mathbf{q}_{n+k-2} + \vartheta \mathbf{e}_{n+k-2}^{\mathbf{q}}, \dot{\mathbf{q}}_{n+k-2} + \vartheta \mathbf{e}_{n+k-2}^{\dot{\mathbf{q}}}, \boldsymbol{\lambda}_{n+k-2} + \vartheta \mathbf{e}_{n+k-2}^{\boldsymbol{\lambda}}, t_{n+k-2})\,\mathbf{e}_{n+k-2}^{\boldsymbol{\lambda}}\,\mathrm{d}\vartheta + \\
&\qquad\qquad + \mathcal{O}(1)(\|\mathbf{e}_{n+k-2}^{\mathbf{q}}\| + \|\mathbf{e}_{n+k-2}^{\dot{\mathbf{q}}}\|) \\
&= \mathbf{g}_{\boldsymbol{\lambda}}(t_n)\,\mathbf{e}_{n+k-2}^{\boldsymbol{\lambda}} + \mathcal{O}(h)\|\mathbf{e}_{n+k-2}^{\boldsymbol{\lambda}}\| + \mathcal{O}(1)(\|\mathbf{e}_{n+k-2}^{\mathbf{q}}\| + \|\mathbf{e}_{n+k-2}^{\dot{\mathbf{q}}}\|) \quad (35)
\end{aligned}
$$

since $\mathbf{q}_{n+k-2} + \vartheta \mathbf{e}_{n+k-2}^{\mathbf{q}} = \mathbf{q}(t_{n+k-2}) + \mathcal{O}(h) = \mathbf{q}(t_n) + \mathcal{O}(h)$ etc., see Equation (34). As before, the notation $\mathbf{g}_{\boldsymbol{\lambda}}(t_n)$ is used as abbreviation for $\mathbf{g}_{\boldsymbol{\lambda}}(\mathbf{q}(t_n), \dot{\mathbf{q}}(t_n), \boldsymbol{\lambda}(t_n), t_n)$.

The matrix product $\boldsymbol{\Phi}_{\mathbf{q}}(\mathbf{q}(t_n), t_n)\,\mathbf{g}_{\boldsymbol{\lambda}}(t_n)$ is non-singular by the index-3 assumption, see Equations (11)-(13). Therefore, the estimate for $\sum_k b_k' \mathbf{e}_{n+k-2}^{\boldsymbol{\lambda}}$ may be obtained multiplying Equation (35) by $[(\boldsymbol{\Phi}_{\mathbf{q}}\mathbf{g}_{\boldsymbol{\lambda}})^{-1}\boldsymbol{\Phi}_{\mathbf{q}}](\mathbf{q}(t_n), t_n)$ from the left and using the error recursion for $\mathbf{e}_n^{\mathbf{g}}$

from Equation (30):

$$\sum_{k=0}^{3} b'_k \mathbf{e}^{\boldsymbol{\lambda}}_{n+k-2} =$$

$$= [(\boldsymbol{\Phi_q g_\lambda})^{-1}\boldsymbol{\Phi_q}](\mathbf{q}(t_n),t_n) \cdot \sum_{k=0}^{3} b'_k \mathbf{e}^{\mathbf{g}}_{n+k-2} + \mathcal{O}(1)\sum_{k=0}^{3}(\|\mathbf{e}^{\mathbf{q}}_{n+k-2}\| + \|\mathbf{e}^{\dot{\mathbf{q}}}_{n+k-2}\| + h\|\mathbf{e}^{\boldsymbol{\lambda}}_{n+k-2}\|)$$

$$= \mathcal{O}(1)\,\|\boldsymbol{\Phi_q}(\mathbf{q}(t_n),t_n) \cdot \frac{1}{h}\sum_{k=0}^{2} a_k \mathbf{e}^{\mathbf{q}'}_{n+k-1}\| + \mathcal{O}(\frac{1}{h})\,\|\mathbf{l}^{\mathbf{q}'}_n\| + \tag{36}$$

$$+ \mathcal{O}(1)\sum_{k=0}^{3}(\|\mathbf{e}^{\mathbf{q}}_{n+k-2}\| + \|\mathbf{e}^{\dot{\mathbf{q}}}_{n+k-2}\| + h\|\mathbf{e}^{\boldsymbol{\lambda}}_{n+k-2}\|)\,.$$

With Lemma 3, see Section 4 below, we get

$$\sum_{k=0}^{3} b'_k \mathbf{e}^{\boldsymbol{\lambda}}_{n+k-2} = \mathcal{O}(\frac{1}{h^2})\sum_{k=0}^{3}\|\boldsymbol{\Phi}(\mathbf{q}_{n+k-2},t_{n+k-2})\| + \mathcal{O}(\frac{1}{h})\,\|\mathbf{l}^{\mathbf{q}'}_n\| +$$

$$+ \mathcal{O}(1)\sum_{k=0}^{3}(\|\mathbf{e}^{\mathbf{q}}_{n+k-2}\| + \|\mathbf{e}^{\dot{\mathbf{q}}}_{n+k-2}\| + h\|\mathbf{e}^{\boldsymbol{\lambda}}_{n+k-2}\|) + \mathcal{O}(1)\sum_{k=0}^{2}\|\mathbf{e}^{\mathbf{q}'}_{n+k-1}\|\,.$$

$$\tag{37}$$

The equilibrium conditions at $t = t_{n+k-2}$ enforce $\boldsymbol{\Phi}(\mathbf{q}_{n+k-2},t_{n+k-2}) = 0$ and Equation (37) may be summarized in the compact form

$$\mathbf{e}^{\boldsymbol{\lambda}}_{n+1} = -\frac{b'_0}{b'_3}\mathbf{e}^{\boldsymbol{\lambda}}_{n-2} - \frac{b'_1}{b'_3}\mathbf{e}^{\boldsymbol{\lambda}}_{n-1} - \frac{b'_2}{b'_3}\mathbf{e}^{\boldsymbol{\lambda}}_n + \mathcal{O}(1)\sum_{k=0}^{3}\|\mathbf{e}^{\mathbf{v}}_{n+k-2}\| + \mathcal{O}(h)\sum_{k=0}^{3}\|\mathbf{e}^{\boldsymbol{\lambda}}_{n+k-2}\| + \mathcal{O}(h^2) \tag{38}$$

The propagation of the errors $\mathbf{e}^{\boldsymbol{\lambda}}_n$ is dominated by the recursion coefficients b'_0, b'_1, b'_2 and b'_3 and it is coupled with the errors $\mathbf{e}^{\mathbf{v}}_n$ in the differential components $\mathbf{q}$, $\dot{\mathbf{q}}$, $\mathbf{q}'$ by $\mathcal{O}(1)$ coupling coefficients.

We note that the terms $\|\boldsymbol{\Phi}(\mathbf{q}_{n+k-2},t_{n+k-2})\|/h^2$ in Equation (37) vanish in the formal convergence analysis but may cause severe problems in a practical implementation of the method. Stopping the Newton iteration in Algorithm 1 with non-zero residuals $\mathbf{r}^{\mathbf{q}}$, $\mathbf{r}^{\boldsymbol{\lambda}}$ may introduce small errors in $\|\boldsymbol{\Phi}(\mathbf{q}_{n+k-2},t_{n+k-2})\|$ that are amplified by the large factor $1/h^2$ during time integration [1]. Therefore, the scaling method of Bottasso et al [3] was used in the numerical tests of Section 5 to keep $\|\boldsymbol{\Phi}(\mathbf{q}_{n+k-2},t_{n+k-2})\|$ as small as possible, see also [13].

3.4 Synthesis

The error propagation in multistep methods may be studied in compact form writing the multistep method as one-step method in a higher dimensional configuration space [12].

With the error vectors

$$\mathbf{E}^{\mathbf{v}}_n = \begin{pmatrix} \mathbf{e}^{\mathbf{v}}_n \\ \mathbf{e}^{\mathbf{v}}_{n-1} \\ \mathbf{e}^{\mathbf{v}}_{n-2} \end{pmatrix}, \quad \mathbf{E}^{\boldsymbol{\lambda}}_n = \begin{pmatrix} \mathbf{e}^{\boldsymbol{\lambda}}_n \\ \mathbf{e}^{\boldsymbol{\lambda}}_{n-1} \\ \mathbf{e}^{\boldsymbol{\lambda}}_{n-2} \end{pmatrix},$$

the propagation relations in Equations (33) and (38) get the form

$$\mathbf{E}^{\mathbf{v}}_{n+1} = \mathbf{A}\,\mathbf{E}^{\mathbf{v}}_n + \mathcal{O}(h)(\|\mathbf{E}^{\mathbf{v}}_n\| + \|\mathbf{E}^{\boldsymbol{\lambda}}_n\|) + \mathcal{O}(h^3)\,, \tag{39}$$

$$\mathbf{E}^{\boldsymbol{\lambda}}_{n+1} = \mathbf{B}'\,\mathbf{E}^{\boldsymbol{\lambda}}_n + \mathcal{O}(1)\|\mathbf{E}^{\mathbf{v}}_n\| + \mathcal{O}(h)\|\mathbf{E}^{\boldsymbol{\lambda}}_n\| + \mathcal{O}(h^2) \tag{40}$$

with error amplification matrices

$$\mathbf{A} = \begin{pmatrix} -\dfrac{a_1}{a_2}\mathbf{I} & -\dfrac{a_0}{a_2}\mathbf{I} & \mathbf{0} \\ \mathbf{I} & \mathbf{0} & \mathbf{0} \\ \mathbf{0} & \mathbf{I} & \mathbf{0} \end{pmatrix} \quad \text{and} \quad \mathbf{B}' = \begin{pmatrix} -\dfrac{b'_2}{b'_3}\mathbf{I} & -\dfrac{b'_1}{b'_3}\mathbf{I} & -\dfrac{b'_0}{b'_3}\mathbf{I} \\ \mathbf{I} & \mathbf{0} & \mathbf{0} \\ \mathbf{0} & \mathbf{I} & \mathbf{0} \end{pmatrix}.$$

In the unconstrained case, zero stability of the multistep method implies $\|\mathbf{A}\| = 1$ in a suitable norm $\|.\|$ and second-order convergence follows by standard arguments from $\|\mathbf{E}_{n+1}^{\mathbf{v}}\| \leq (1 + \mathcal{O}(h))\|\mathbf{E}_n^{\mathbf{v}}\| + \mathcal{O}(h^3)$, see [12].

In the constrained case, a similar argument is used to show that strict stability at infinity implies $\|\mathbf{B}'\| < 1$ in a (possibly different) norm $\|.\|$ for the algebraic solution components [13]. More precisely, the method is strictly stable at infinity if the roots ζ_i', $i = 1, 2, 3$, of the polynomial σ in Equation (22) are bounded by $\zeta_{\max}' := \max_i |\zeta_i'| < 1$, see Lemma 1 below, and $\|\mathbf{B}'\| = \rho < 1$ may be achieved for any $\rho > \zeta_{\max}'$ using an appropriate norm $\|.\|$ for the algebraic components [13].

Taking norms in Equations (39) and (40), we obtain

$$
\left(\begin{array}{c} \|\mathbf{E}_{n+1}^{\mathbf{v}}\| \\ \|\mathbf{E}_{n+1}^{\boldsymbol{\lambda}}\| \end{array} \right) \leq \left(\begin{array}{cc} 1 + \mathcal{O}(h) & \mathcal{O}(h) \\ \mathcal{O}(1) & \rho + \mathcal{O}(h) \end{array} \right) \left(\begin{array}{c} \|\mathbf{E}_n^{\mathbf{v}}\| \\ \|\mathbf{E}_n^{\boldsymbol{\lambda}}\| \end{array} \right) + \left(\begin{array}{c} \mathcal{O}(h^3) \\ \mathcal{O}(h^2) \end{array} \right)
$$

and we deduce, as in [13], that the global errors after n steps satisfy

$$
\left(\begin{array}{c} \|\mathbf{E}_n^{\mathbf{v}}\| \\ \|\mathbf{E}_n^{\boldsymbol{\lambda}}\| \end{array} \right) = \mathcal{O}(1)\|\mathbf{E}_0^{\mathbf{v}}\| + (\mathcal{O}(h) + \mathcal{O}(1)\rho^n)\|\mathbf{E}_0^{\boldsymbol{\lambda}}\| + \mathcal{O}(h^2). \tag{41}
$$

Note, that strict stability at infinity allows to prove second-order convergence for *all* solution components despite the local error $\mathcal{O}(h^2)$ in the algebraic solution components, see Equation (40). Furthermore, $\rho < 1$ implies also that errors $\mathbf{E}_0^{\boldsymbol{\lambda}}$ in the initial values of the Lagrange multipliers are damped out rapidly.

Summary In the constrained case, the generalized-α method with fixed time step-size h has global errors $\mathcal{O}(h^2)$ in $\mathbf{q}$, $\dot{\mathbf{q}}$ and $\boldsymbol{\lambda}$ if the order 2 condition in Equation (20) and the stability conditions in Equation (23) are satisfied and the errors $\mathbf{E}_0^{\mathbf{v}}$, $\mathbf{E}_0^{\boldsymbol{\lambda}}$ in the initial values are $\mathcal{O}(h^2)$. The CH-α algorithm with $\rho_\infty \in [0, 1)$, see Equation (24), may be considered as a typical example of a second-order convergent method for constrained systems.

4 Technical details of the error estimates

In the present section, some technical details of the convergence analysis are summarized. Readers, who are mainly interested in the basic steps of the analysis, may skip this section and continue with the results of numerical tests in Section 5 below.

Lemma 1 *A generalized-α scheme with parameters that satisfy the order 2 condition in Equation (20) and the stability conditions in Equation (23) is strictly stable at infinity, i.e., all roots ζ_i' of polynomial $\sigma(\zeta)$, see Equation (22), are inside the unit circle: $|\zeta_i'| < 1$, $i = 1, 2, 3$.*

Proof: Polynomial $\sigma(\zeta)$ may be written as

$$
\sigma(\zeta) = \sum_{k=0}^3 b_k' \zeta^k = \beta \left((1 - \alpha_f)\zeta + \alpha_f \right) \left(\zeta^2 + \frac{\frac{1}{2} + \gamma - 2\beta}{\beta}\zeta + \frac{\frac{1}{2} - \gamma + \beta}{\beta} \right)
$$

with roots

$$
\zeta_1' = -\frac{\alpha_f}{1 - \alpha_f}, \quad \zeta_{2,3}' = -\frac{\frac{1}{2} + \gamma - 2\beta}{2\beta} \pm \frac{R}{2\beta} \quad \text{and} \quad R := \left((\frac{1}{2} + \gamma - 2\beta)^2 - 4\beta(\frac{1}{2} - \gamma + \beta) \right)^{1/2}.
$$

Because of $\alpha_f < 1/2$ we get $|\zeta_1'| < 1$, see Equation (23).

If the roots ζ_2', ζ_3' are complex, we have $\zeta_2' = \bar{\zeta}_3'$ and Vieta's Theorem implies

$$
|\zeta_2'| = |\zeta_3'| = (\zeta_2'\zeta_3')^{1/2} = \left(\frac{\frac{1}{2} - \gamma + \beta}{\beta} \right)^{1/2} < \left(\frac{\beta}{\beta} \right)^{1/2} = 1
$$

9

since $\alpha_m < \alpha_f \Rightarrow \gamma > 1/2$, see Equation (20).

For real roots ζ_2', ζ_3', we observe

$$R^2 = (\frac{1}{2} + \gamma)^2 - 4\beta < (\frac{1}{2} + \gamma)^2 \Rightarrow R < \frac{1}{2} + \gamma\,,$$

$$R^2 = \left(4\beta - (\frac{1}{2} + \gamma)\right)^2 - 8\beta(2\beta - \gamma) < \left(4\beta - (\frac{1}{2} + \gamma)\right)^2 \Rightarrow -R > -\left(4\beta - (\frac{1}{2} + \gamma)\right)$$

since $2\beta - \gamma > 0$ and $4\beta - (\frac{1}{2} + \gamma) = 2(\beta - \frac{1}{4}) + (2\beta - \gamma) > 0$, see Equations (20) and (23).

Therefore, real roots ζ_2', ζ_3' are bounded by

$$\zeta_{2,3}' \; < \; -\frac{\frac{1}{2} + \gamma - 2\beta}{2\beta} + \frac{\frac{1}{2} + \gamma}{2\beta} = \frac{2\beta}{2\beta} = 1\,,$$

$$\zeta_{2,3}' \; > \; -\frac{\frac{1}{2} + \gamma - 2\beta}{2\beta} - \frac{4\beta - (\frac{1}{2} + \gamma)}{2\beta} = -\frac{2\beta}{2\beta} = -1$$

and $|\zeta_i'| < 1$, $i = 1, 2, 3$ is guaranteed also in that case. ∎

Lemma 2 *For vectors* $\mathbf{q}_{n+k-2}$ *with* $\|\mathbf{e}_{n+k-2}^{\mathbf{q}}\| = \mathcal{O}(h)$, $k = 0, 1, 2, 3$, *the terms* $\boldsymbol{\Phi}_{\mathbf{q}}(\mathbf{q}(t_n), t_n)\mathbf{e}_{n+k-1}^{\mathbf{q}'}$, $k = 0, 1, 2$, *satisfy (the arguments* t *in* $\boldsymbol{\Phi}$ *and* $\boldsymbol{\Phi}_{\mathbf{q}}$ *are omitted for simplicity)*

$$\boldsymbol{\Phi}_{\mathbf{q}}(\mathbf{q}(t_n))\mathbf{e}_{n+k-1}^{\mathbf{q}'} = \frac{1}{h}\left(\boldsymbol{\Phi}(\mathbf{q}_{n+k-2}) - \boldsymbol{\Phi}(\mathbf{q}_{n+k-1})\right) - \frac{\partial}{\partial \mathbf{q}}\left(\boldsymbol{\Phi}_{\mathbf{q}}(\mathbf{q})\,\mathbf{e}_{n+k-2}^{\mathbf{q}}\right)\Big|_{\mathbf{q}=\mathbf{q}(t_n)} \cdot \dot{\mathbf{q}}(t_n) +$$

$$+ \mathcal{O}(h)\left(\|\mathbf{e}_{n+k-1}^{\mathbf{q}}\| + \|\mathbf{e}_{n+k-2}^{\mathbf{q}}\| + \|\mathbf{e}_{n+k-1}^{\mathbf{q}'}\|\right), \quad (h \to 0)\,. \tag{42}$$

Proof: To keep notation compact, the proof is given for $k = 2$ and the argument t in $\boldsymbol{\Phi}(\mathbf{q}, t)$ is omitted. The extension to $k = 0, 1$ and to $\boldsymbol{\Phi} = \boldsymbol{\Phi}(\mathbf{q}, t)$ is straightforward.

For linear time-invariant constraints $\boldsymbol{\Phi}(\mathbf{q}(t)) = \mathbf{C}\mathbf{q}(t) - \mathbf{z} = \mathbf{0}$, the proposition of the lemma is trivial since $\boldsymbol{\Phi}_{\mathbf{q}} \equiv \mathbf{C}$, $\boldsymbol{\Phi}_{\mathbf{q}\mathbf{q}} \equiv \mathbf{0}$ and $\mathbf{e}_{n+1}^{\mathbf{q}'} = (\mathbf{e}_{n+1}^{\mathbf{q}} - \mathbf{e}_n^{\mathbf{q}})/h$, see Equation (31):

$$\mathbf{C}\mathbf{e}_{n+1}^{\mathbf{q}'} = \mathbf{C}\left(\frac{\mathbf{q}(t_{n+1}) - \mathbf{q}(t_n)}{h} - \frac{\mathbf{q}_{n+1} - \mathbf{q}_n}{h}\right) = \frac{\mathbf{z} - \mathbf{z}}{h} - \frac{(\boldsymbol{\Phi}(\mathbf{q}_{n+1}) + \mathbf{z}) - (\boldsymbol{\Phi}(\mathbf{q}_n) + \mathbf{z})}{h}\,.$$

In the nonlinear case, the identity

$$-\boldsymbol{\Phi}(\mathbf{q}_n) = \boldsymbol{\Phi}(\mathbf{q}(t_n)) - \boldsymbol{\Phi}(\mathbf{q}_n) = \int_0^1 \boldsymbol{\Phi}_{\mathbf{q}}(\mathbf{q}_n + \vartheta\mathbf{e}_n^{\mathbf{q}})\mathbf{e}_n^{\mathbf{q}}\,\mathrm{d}\vartheta \tag{43}$$

is used that follows from

$$\boldsymbol{\psi}(1) - \boldsymbol{\psi}(0) = \int_0^1 \boldsymbol{\psi}'(\vartheta)\,\mathrm{d}\vartheta \quad \text{with} \quad \boldsymbol{\psi}(\vartheta) := \boldsymbol{\Phi}(\mathbf{q}_n + \vartheta\mathbf{e}_n^{\mathbf{q}})\,, \;\; \boldsymbol{\psi}'(\vartheta) = \boldsymbol{\Phi}_{\mathbf{q}}(\mathbf{q}_n + \vartheta\mathbf{e}_n^{\mathbf{q}})\mathbf{e}_n^{\mathbf{q}}\,.$$

Because of Equation (43) and the corresponding identity with n being substituted by $n + 1$ we have

$$\frac{1}{h}\left(\boldsymbol{\Phi}(\mathbf{q}_n) - \boldsymbol{\Phi}(\mathbf{q}_{n+1})\right) =$$

$$= \frac{1}{h}\int_0^1 \boldsymbol{\Phi}_{\mathbf{q}}(\mathbf{q}_{n+1} + \vartheta\mathbf{e}_{n+1}^{\mathbf{q}})\mathbf{e}_{n+1}^{\mathbf{q}}\,\mathrm{d}\vartheta - \frac{1}{h}\int_0^1 \boldsymbol{\Phi}_{\mathbf{q}}(\mathbf{q}_n + \vartheta\mathbf{e}_n^{\mathbf{q}})\mathbf{e}_n^{\mathbf{q}}\,\mathrm{d}\vartheta$$

$$= \int_0^1 \boldsymbol{\Phi}_{\mathbf{q}}(\mathbf{q}_{n+1} + \vartheta\mathbf{e}_{n+1}^{\mathbf{q}})\mathbf{e}_{n+1}^{\mathbf{q}'}\,\mathrm{d}\vartheta + \frac{1}{h}\int_0^1 \left(\boldsymbol{\Phi}_{\mathbf{q}}(\mathbf{q}_{n+1} + \vartheta\mathbf{e}_{n+1}^{\mathbf{q}}) - \boldsymbol{\Phi}_{\mathbf{q}}(\mathbf{q}_n + \vartheta\mathbf{e}_n^{\mathbf{q}})\right)\mathbf{e}_n^{\mathbf{q}}\,\mathrm{d}\vartheta \tag{44}$$

since $(\mathbf{e}^{\mathbf{q}}_{n+1} - \mathbf{e}^{\mathbf{q}}_n)/h = \mathbf{e}^{\mathbf{q}'}_{n+1}$. The first term in the right hand side of Equation (44) may be written as

$$\int_0^1 \boldsymbol{\Phi}_{\mathbf{q}}(\mathbf{q}_{n+1} + \vartheta \mathbf{e}^{\mathbf{q}}_{n+1})\mathbf{e}^{\mathbf{q}'}_{n+1}\,\mathrm{d}\vartheta = \boldsymbol{\Phi}_{\mathbf{q}}(\mathbf{q}(t_n))\mathbf{e}^{\mathbf{q}'}_{n+1} + \mathcal{O}(h)\|\mathbf{e}^{\mathbf{q}'}_{n+1}\| \tag{45}$$

because $\mathbf{q}_{n+1} + \vartheta \mathbf{e}^{\mathbf{q}}_{n+1} = \mathbf{q}(t_{n+1}) + \mathcal{O}(h) = \mathbf{q}(t_n) + \mathcal{O}(h)$.

The second term in Equation (44) contains curvature terms $\boldsymbol{\Phi}_{\mathbf{qq}}$. It vanishes in the linear time-invariant case but needs special care for nonlinear constraints. The term may be expressed as

$$\frac{1}{h}\int_0^1 \Big(\boldsymbol{\psi}(1;\vartheta) - \boldsymbol{\psi}(0;\vartheta)\Big)\,\mathrm{d}\vartheta \tag{46}$$

with $\boldsymbol{\psi}(\bar{\vartheta};\vartheta) := \boldsymbol{\Phi}_{\mathbf{q}}(\bar{\mathbf{q}}(\bar{\vartheta};\vartheta))\mathbf{e}^{\mathbf{q}}_n$ and generalized coordinates

$$\bar{\mathbf{q}}(\bar{\vartheta};\vartheta) := \mathbf{q}_n + \bar{\vartheta}(\mathbf{q}_{n+1} - \mathbf{q}_n) + \vartheta\Big(\mathbf{e}^{\mathbf{q}}_n + \bar{\vartheta}(\mathbf{e}^{\mathbf{q}}_{n+1} - \mathbf{e}^{\mathbf{q}}_n)\Big) = \mathbf{q}(t_n) + \mathcal{O}(h)\,.$$

With these notations, we get in Equation (46)

$$\frac{1}{h}\int_0^1 \Big(\boldsymbol{\psi}(1;\vartheta) - \boldsymbol{\psi}(0;\vartheta)\Big)\,\mathrm{d}\vartheta = \frac{1}{h}\int_0^1\int_0^1 \frac{\partial}{\partial\bar{\vartheta}}\boldsymbol{\psi}(\bar{\vartheta};\vartheta)\,\mathrm{d}\bar{\vartheta}\,\mathrm{d}\vartheta =$$

$$= \frac{1}{h}\int_0^1\int_0^1 \frac{\partial}{\partial\mathbf{q}}\Big(\boldsymbol{\Phi}(\mathbf{q})\mathbf{e}^{\mathbf{q}}_n\Big)\Big|_{\mathbf{q}=\bar{\mathbf{q}}(\bar{\vartheta};\vartheta)} \cdot \frac{\partial}{\partial\bar{\vartheta}}\bar{\mathbf{q}}(\bar{\vartheta};\vartheta)\,\mathrm{d}\bar{\vartheta}\,\mathrm{d}\vartheta$$

$$= \int_0^1\int_0^1 \frac{\partial}{\partial\mathbf{q}}\Big(\boldsymbol{\Phi}(\mathbf{q})\mathbf{e}^{\mathbf{q}}_n\Big)\Big|_{\mathbf{q}=\bar{\mathbf{q}}(\bar{\vartheta};\vartheta)} \cdot \dot{\mathbf{q}}(t_n)\,\mathrm{d}\bar{\vartheta}\,\mathrm{d}\vartheta + \mathcal{O}(\|\mathbf{e}^{\mathbf{q}}_n\|)\cdot\max_{\vartheta,\bar{\vartheta}}\|\frac{1}{h}\frac{\partial}{\partial\bar{\vartheta}}\bar{\mathbf{q}}(\bar{\vartheta};\vartheta) - \dot{\mathbf{q}}(t_n)\|$$

$$= \int_0^1\int_0^1 \frac{\partial}{\partial\mathbf{q}}\Big(\boldsymbol{\Phi}(\mathbf{q})\mathbf{e}^{\mathbf{q}}_n\Big)\Big|_{\mathbf{q}=\mathbf{q}(t_n)} \cdot \dot{\mathbf{q}}(t_n)\,\mathrm{d}\bar{\vartheta}\,\mathrm{d}\vartheta + \mathcal{O}(h)\|\mathbf{e}^{\mathbf{q}}_n\| +$$

$$+ \mathcal{O}(\|\mathbf{e}^{\mathbf{q}}_n\|)\cdot\max_{\vartheta,\bar{\vartheta}}\|\frac{\mathbf{q}(t_{n+1}) - \mathbf{q}(t_n)}{h} - (1-\vartheta)\mathbf{e}^{\mathbf{q}'}_{n+1} - \dot{\mathbf{q}}(t_n)\|$$

$$= \frac{\partial}{\partial\mathbf{q}}\Big(\boldsymbol{\Phi}(\mathbf{q})\mathbf{e}^{\mathbf{q}}_n\Big)\Big|_{\mathbf{q}=\mathbf{q}(t_n)} \cdot \dot{\mathbf{q}}(t_n) + \mathcal{O}(h)\|\mathbf{e}^{\mathbf{q}}_n\| + \mathcal{O}(h)\|\mathbf{e}^{\mathbf{q}'}_{n+1}\| \tag{47}$$

since $\|\mathbf{e}^{\mathbf{q}}_n\| = \mathcal{O}(h)$ by assumption and $\mathbf{q}(t_{n+1}) - \mathbf{q}(t_n) = h\dot{\mathbf{q}}(t_n) + \mathcal{O}(h^2)$. The proof is completed substituting Equations (45)–(47) in Equation (44). ■

Lemma 3 *With the assumptions of Lemma 2, the first term in the right hand side of Equation (36) satisfies (the arguments t in $\boldsymbol{\Phi}$ and $\boldsymbol{\Phi}_{\mathbf{q}}$ are again omitted):*

$$\boldsymbol{\Phi}_{\mathbf{q}}(\mathbf{q}(t_n))\cdot\frac{1}{h}\sum_{k=0}^{2} a_k \mathbf{e}^{\mathbf{q}'}_{n+k-1} = \mathcal{O}(\frac{1}{h^2})\sum_{k=0}^{3}\|\boldsymbol{\Phi}(\mathbf{q}_{n+k-2})\| + \mathcal{O}(1)\Big(\sum_{k=0}^{3}\|\mathbf{e}^{\mathbf{q}}_{n+k-2}\| + \sum_{k=0}^{2}\|\mathbf{e}^{\mathbf{q}'}_{n+k-1}\|\Big)\,. \tag{48}$$

Proof: The one-step nature of the generalized-α scheme results in a very special multistep representation of the error recursion in components $\mathbf{q}'_n$ because $a_1 = -1 + 2\alpha_m = -(1-\alpha_m) + \alpha_m = -a_2 - a_0$:

$$\frac{1}{h}\sum_{k=0}^{2} a_k \mathbf{e}^{\mathbf{q}'}_{n+k-1} = (1-\alpha_m)\frac{\mathbf{e}^{\mathbf{q}'}_{n+1} - \mathbf{e}^{\mathbf{q}'}_n}{h} + \alpha_m\frac{\mathbf{e}^{\mathbf{q}'}_n - \mathbf{e}^{\mathbf{q}'}_{n-1}}{h}\,. \tag{49}$$

Multiplying Equation (49) by $\boldsymbol{\Phi}_{\mathbf{q}}(\mathbf{q}(t_n))$ and applying Lemma 2 to

$$\boldsymbol{\Phi}_{\mathbf{q}}(\mathbf{q}(t_n))\frac{\mathbf{e}^{\mathbf{q}'}_{n+k-1} - \mathbf{e}^{\mathbf{q}'}_{n+k-2}}{h} = \frac{1}{h}\boldsymbol{\Phi}_{\mathbf{q}}(\mathbf{q}(t_n))\mathbf{e}^{\mathbf{q}'}_{n+k-1} - \frac{1}{h}\boldsymbol{\Phi}_{\mathbf{q}}(\mathbf{q}(t_n))\mathbf{e}^{\mathbf{q}'}_{n+k-2}\,,\quad (k=1,2)\,,$$

11

we see that the estimate in Equation (48) is a straightforward consequence of Equation (49), Lemma 2 and

$$-\frac{\partial}{\partial \mathbf{q}}\left(\mathbf{\Phi}(\mathbf{q})\frac{\mathbf{e}_{n+k-2}^{\mathbf{q}} - \mathbf{e}_{n+k-3}^{\mathbf{q}}}{h}\right)\Big|_{\mathbf{q}=\mathbf{q}(t_n)}\cdot\dot{\mathbf{q}}(t_n) = -\frac{\partial}{\partial \mathbf{q}}\left(\mathbf{\Phi}(\mathbf{q})\mathbf{e}_{n+k-2}^{\mathbf{q}'}\right)\Big|_{\mathbf{q}=\mathbf{q}(t_n)}\cdot\dot{\mathbf{q}}(t_n) = \mathcal{O}(\|\mathbf{e}_{n+k-2}^{\mathbf{q}'}\|)$$

for $k = 1, 2$. ∎

5 Numerical tests

The following numerical tests have been developed in the formalism described by Géradin and Cardona [11], which allows to account for flexible bodies. Hence, the equations of motion are obtained in terms of absolute nodal coordinates with respect to the inertial frame.

5.1 Slider-crank mechanism

The first example is a slider-crank mechanism with a spring-mass system attached to the sliding body, see Figure 1. A similar benchmark has been considered in [16]. This planar system has two degrees-of-freedom that can be represented by the crank angle θ_1 and the displacement of the additional mass x_4. The model involves 10 generalized coordinates: the positions of the centers of mass of body 1 and 2, (x_1, y_1, x_2, y_2), their orientation (θ_1, θ_2), the position of bodies 3 and 4 (x_3, x_4) and the position of the hinge connecting body 1 and 2 (x_5, y_5). This set of coordinates has to satisfy 8 nonlinear kinematic constraints.

The spring stiffness is $k = 1000$ N/m, the length of bodies 1 and 2 are $l_1 = 0.3$ m and $l_2 = 0.6$ m and the masses are $m_1 = 0.36$ kg, $m_2 = 0.15$ kg, $m_3 = 0.1$ kg and $m_4 = 0.7$ kg. Initially, $\theta_1 = \pi/2$, the spring is undeformed and the mechanism is at rest. A constant torque $T = 1$ Nm is applied to the crank and the initial conditions are computed so that the constraints are satisfied at position, velocity and acceleration level. The parameters of the generalized-α algorithm have been selected according to Equation (24). The spectral radius of the algorithm is set to the typical value $\rho_\infty = 0.7$, which leads to a sufficient amount of high-frequency numerical dissipation for the problem at hand. For a time step $h = 5.e-3$ s, the numerical results are given in Figure 2.

A convergence study has been realized for $h \to 0$ and the results are plotted in Figure 3. The reference solution has been computed using a smaller time step. Second-order convergence is observed both for the generalized coordinates and the Lagrange multipliers.

5.2 Andrews' mechanism

Andrews' squeezing mechanism, which is represented in Figure 4, consists of seven articulated rigid bodies moving in a plane. This standard benchmark, described in details by Schiehlen [19], has been largely exploited to demonstrate the performance of DAE time-integration schemes. The mechanism has only one degree-of-freedom, and a constant torque is applied at point O. In the original benchmark, the equations of motion are explicitly given in terms of relative
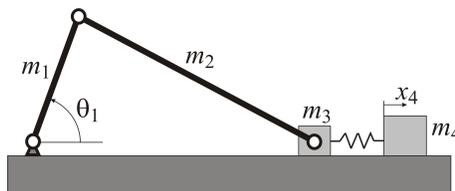

Figure 1: Slider-crank mechanism.
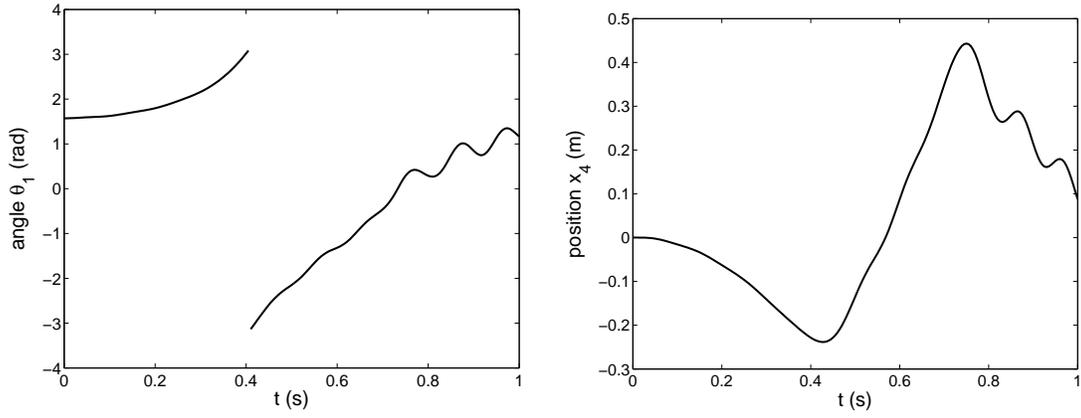
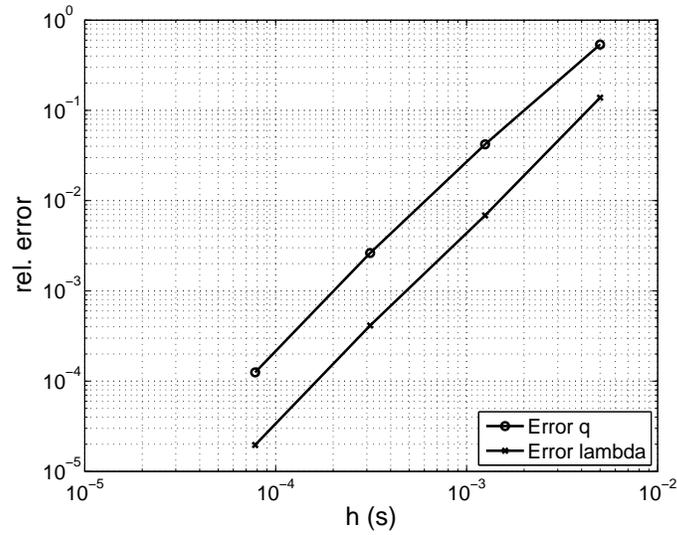Figure 2: Crank angle θ_1 and position of the additional mass x_4.

Figure 3: Convergence of relative errors at final time ($t = 1$ s) for a generalized coordinates (θ_1) and a Lagrange multiplier (λ_1).
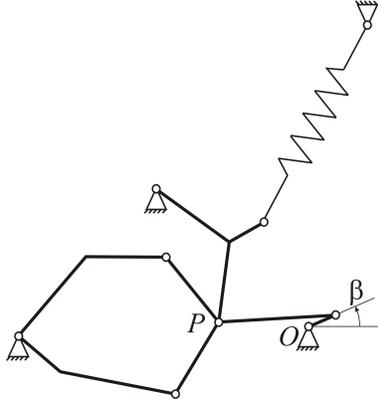
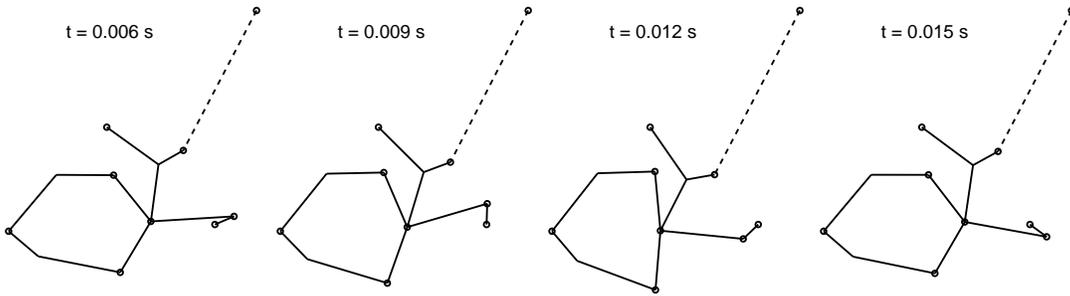Figure 4: Andrews' squeezing mechanism.

Figure 5: Motion snapshots of the squeezing mechanism.

coordinates. In this work, one absolute rotation is defined for each body, whereas two translation coordinates are defined for each moving joint and each center of mass. Hence, the model involves a total of 31 generalized coordinates and 30 kinematic constraints. Initially, the mechanism is at rest, and the initial conditions are computed so that the constraints are satisfied at position, velocity and acceleration level.

As in the previous example, the parameters of the generalized-α algorithm have been selected according to Equation (24) with a spectral radius $\rho_\infty = 0.7$. For a time step $h = 3.$e-4 s, the numerical results are illustrated in Figures 5, 6 and 7. Numerical damping is quite important to ensure a stable numerical solution, and a stable error propagation. For instance, Figure 8 gives some results for the undamped algorithm ($\rho_\infty = 1$), which are strongly affected by numerical oscillations.

The results of a convergence analysis are plotted in Figure 9. In the published benchmark, a reference solution is given for the body angles at final time. For the multipliers, we have computed a reference solution using a smaller time step. Second-order convergence is observed both for the generalized coordinates and the Lagrange multipliers. However, for very small h, the Lagrange multipliers are more sensitive to numerical errors.

6 Conclusions

This paper analyses the accuracy of the generalized-α method for constrained mechanical systems. We note that the proposed algorithm, which is a variant of the original generalized-α algorithm, can deal with a non-constant mass matrix and that the accelerations are computed
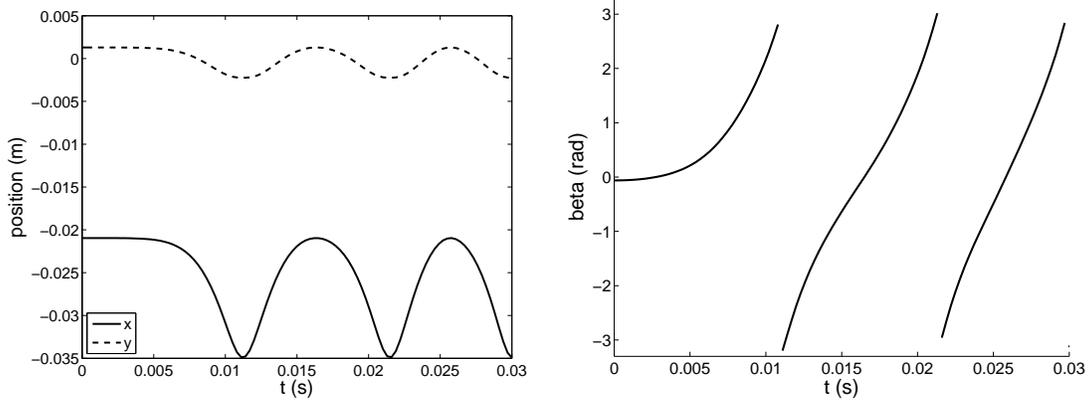
Figure 6: (x, y)-position of point P and angle β.

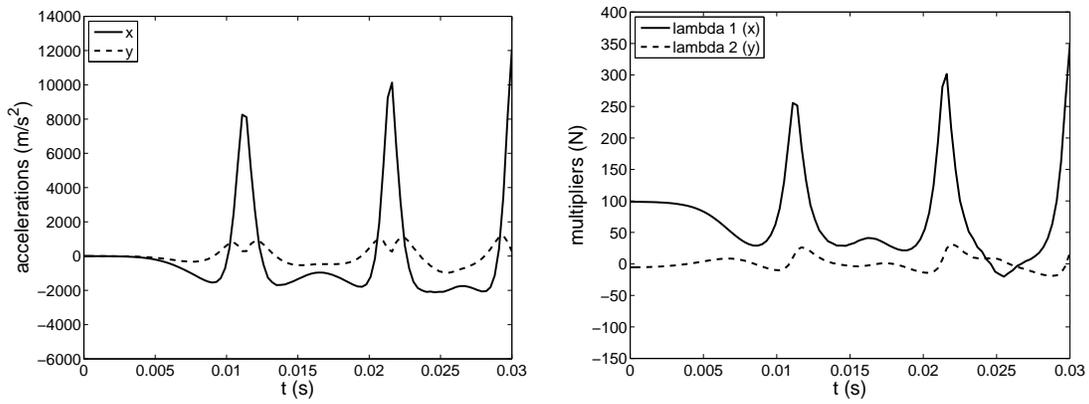

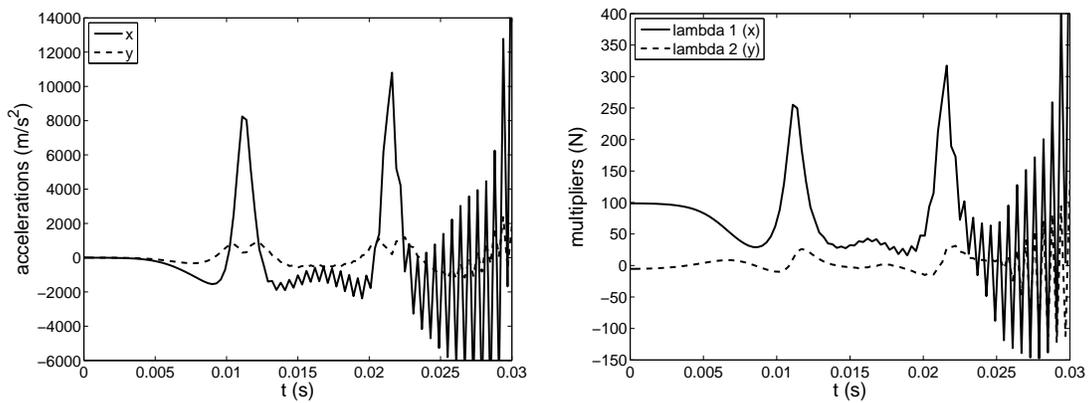Figure 7: (x, y)-accelerations of point P and Lagrange multipliers.

Figure 8: Without numerical damping: (x, y)-accelerations of point P and Lagrange multipliers associated with the (x, y) internal forces in body 1.
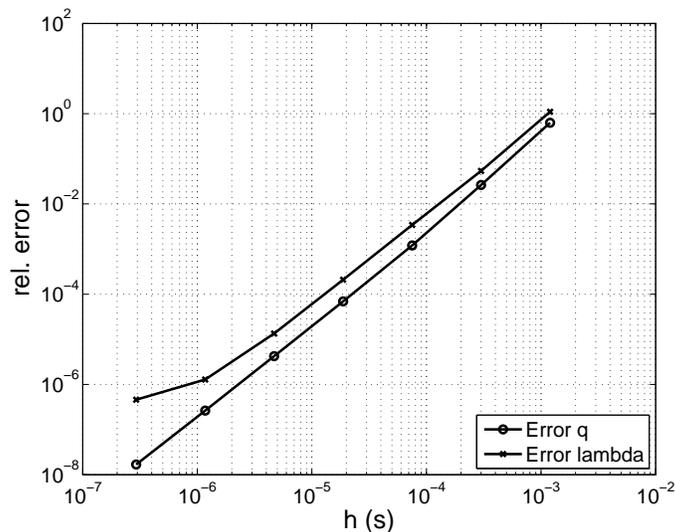
Figure 9: Convergence of relative errors at final time ($t = 0.03$ s) for a generalized coordinates (β) and a Lagrange multiplier (λ_1).

with second-order accuracy.

Using the analogy with multistep algorithms, global second-order convergence has been proven both for the generalized coordinates and the Lagrange multipliers. Those properties have been illustrated by numerical tests.

Acknowledgements

References

[1] Arnold, M.: A perturbation analysis for the dynamical simulation of mechanical multibody systems. Applied Numerical Mathematics **18**, 37–56 (1995)

[2] Arnold, M.: Simulation algorithms and software tools. **accepted for publication in:** G. Mastinu, M. Plöchl (eds.) Road and Off-Road Vehicle System Dynamics Handbook. Taylor & Francis, London (2007, **in preparation**)

[3] Bottasso, C., Dopico, D., Trainelli, L.: On the optimal scaling of index three DAEs in multibody dynamics. In: Proc. of the European Conference on Computational Mechanics (ECCOMAS-ECCM). Lisbon, Portugal (2006)

[4] Brenan, K., Campbell, S., Petzold, L.: Numerical Solution of Initial-Value Problems in Differential-Algebraic Equations, 2nd edn. SIAM, Philadelphia (1996)

[5] Bruls, O., Arnold, M.: The generalized-α scheme as a multistep integrator: Towards a general mechatronic simulator. To appear in: Proc. of the IDETC/MSNDC Conference. Las Vegas, U.S. (2007)

[6] Bruls, O., Golinval, J.C.: The generalized-α method in mechatronic applications. Zeitschrift für Angewandte Mathematik und Mechanik (ZAMM) **86**, 748–758 (2006)

[7] Bruls, O., Golinval, J.C.: On the numerical damping of time integrators for coupled mechatronic systems. Computer Methods in Applied Mechanics and Engineering **accepted for publication** (2006)

[8] Cardona, A., Géradin, M.: Time integration of the equations of motion in mechanism analysis. Computers and Structures **33**, 801–820 (1989)

[9] Chung, J., Hulbert, G.: A time integration algorithm for structural dynamics with improved numerical dissipation: The generalized-α method. ASME Journal of Applied Mechanics **60**, 371–375 (1993)

[10] Erlicher, S., Bonaventura, L., Bursi, O.: The analysis of the generalized-α method for non-linear dynamic problems. Computational Mechanics **28**, 83–104 (2002)

[11] Géradin, M., Cardona, A.: Flexible Multibody Dynamics: A Finite Element Approach. John Wiley & Sons, New York (2001)

[12] Hairer, E., Norsett, S., Wanner, G.: Solving Ordinary Differential Equations I - Nonstiff Problems, 2nd edn. Springer-Verlag (1993)

[13] Hairer, E., Wanner, G.: Solving Ordinary Differential Equations II - Stiff and Differential-Algebraic Problems, 2nd edn. Springer-Verlag (1996)

[14] Hilber, H., Hughes, T., Taylor, R.: Improved numerical dissipation for time integration algorithms in structural dynamics. Earthquake Engineering and Structural Dynamics **5**, 283–292 (1977)

[15] Jay, L., Negrut, D.: Extensions of the HHT-method to differential-algebraic equations in mechanics. Electronic Transactions on Numerical Analysis **26**, 190–208 (2007)

[16] Lunk, C., Simeon, B.: Solving constrained mechanical systems by the family of Newmark and α-methods. Zeitschrift für Angewandte Mathematik und Mechanik (ZAMM) **86**(10), 772–784 (2006)

[17] Negrut, D., Rampalli, R., Ottarsson, G., Sajdak, A.: On the use of the HHT method in the context of index 3 differential algebraic equations of multi-body dynamics. In: J. Goicolea, J. Cuadrado, J. García Orden (eds.) Proc. of the ECCOMAS Conf. on Advances in Computational Multibody Dynamics. Madrid, Spain (2005)

[18] Newmark, N.: A method of computation for structural dynamics. ASCE Journal of the Engineering Mechanics Division **85**, 67–94 (1959)

[19] Schiehlen, W. (ed.): Multibody Systems Handbook. Springer Verlag, Berlin (1990)